

Performance study of a bakelite RPC prototype built by new technique of linseed oil coating

A. Sen^a, S. Chatterjee^b, S. Mandal, S. Das, S. Biswas*

Department of Physical Sciences, Bose Institute, EN-80, Sector V,
Kolkata-700091, India

Abstract

Resistive Plate Chamber (RPC) is one of the most commonly used detectors in high energy physics experiments for triggering and tracking because of its good efficiency ($> 90\%$) and time resolution ($\sim 1-2$ ns). Generally, the bakelite which is one of the most commonly used materials used as electrode plates in RPC, sometimes suffer from surface roughness issues. If the surface is not smooth, the micro discharge probability and spurious pulses increase, which leads to the deterioration in the performance of the detector. We have developed a new method of linseed oil coating for the bakelite based detectors to avoid the surface roughness issue. The detector is characterised with Tetrafluoroethane based gas mixture. The detector is also tested with a high rate of gamma radiation environment in the lab for the radiation hardness test. The detailed measurement procedure and test results are presented in this article.

Keyword: Resistive plate chambers; Bakelite; Linseed oil coating; Long-term test, Charge Sharing; Gamma irradiation

1 Introduction

Resistive Plate Chamber (RPC), first developed by Santonico *et al.* [1] using bakelite, is a gas filled detector used extensively in high energy physics (HEP) experiments for their high efficiency ($> 90\%$) and good time resolution ($\sim 1-2$ ns) [2, 3, 4]. HEP experiments such as BaBar [5], ATLAS

^aNow at Jefferson Lab and Ohio University, Athens, USA

^bNow at University of Massachusetts, Amherst, USA

*Corresponding author.

E-mail: saikat@jcbose.ac.in

[6], ALICE [7] use it for the triggering purpose and experiments like ALICE [8], STAR [9] use it as the tracking device. Cosmic ray experiments like ARGO-YBJ [10], COVER-PLASTEX [11], Daya Bay [12] also use RPC for the muon detection.

The surface of the bakelite electrode plates normally have some microstructure that can cause a high noise rate and low efficiency [13]. In addition to that, this non-uniformity in the electrode surface increases the spark probability and subsequently the leakage current.

To get rid of the surface roughness issue, linseed oil treatment process was already developed some time back [14]. Generally, linseed oil with a thinner solution in some specific ratio is mixed, and the mixture is applied over the bakelite electrode surface as a coating. After the application of the coating, it is completely dried out to cure the electrode plate [15].

But in the BaBar experiment, it was first observed that improper curing of the linseed oil coating gave rise to formation of stalagmite, and the performance of the RPC was drastically reduced [16, 17].

After this incident, numerous R&D on the development of bakelite RPC have been carried out. The problem was finally solved for the linseed oil coated bakelite RPC by using additional thinner with the linseed oil and also using very thin layer of coating [18, 19]. Sometimes, bakelite RPCs have been fabricated without any coating [20]. Coating of some other oil is also used for bakelite RPCs for low rate experiments [21]. We have developed a new technique of linseed oil coating to eliminate the curing issue. In this procedure, oil coating is done before fabricating the detector. The details of the fabrication procedure and the first performance studies are presented elsewhere [22].

Table 1: Summary of previous experimental results

Gas composition	Efficiency (%)	Noise rate (Hz/cm²)	Leakage current @ 10 kV (μA)
100% Tetrafluoroethane (100% C ₂ H ₂ F ₄)	@ - 15 mV threshold 95 \pm 1 from 9.4 kV onwards	500	19
	@ - 20 mV threshold 85 \pm 5 from 10.1 kV onwards	200	
C ₂ H ₂ F ₄ / i-C ₄ H ₁₀ 90/10	@ - 20 mV threshold 95 \pm 2 from 10 kV onwards	120	4.5
	@ - 25 mV threshold 95 \pm 2 from 10 kV onwards	80	

The detector is initially tested with 100% Tetrafluoroethane ($C_2H_2F_4$) gas, and an efficiency $> 90\%$ with higher noise rate compared to the conventional linseed oil-coated detectors is obtained [22]. The detector is further characterised with conventional mixed gas *i.e.* 90% $C_2H_2F_4$ and 10% isobutane ($i-C_4H_{10}$). An efficiency greater than 90% is also found with this mixture but with a lower noise rate [23]. The leakage current is also found to be lower with the mixed gas compared to that with the 100% $C_2H_2F_4$. At a glance, the previously obtained experimental results for two different gas compositions are summarised in Table 1 [22, 23].

Radiation hardness is one of the important factors for detectors in heavy-ion physics experiments. That is why the efficiency and noise rate of the chamber is also measured in the laboratory with a gamma-ray background. In this article, the results of measurement of time resolution and long-term stability test are presented along with the result of the radiation hardness test.

2 Construction of the chamber

The electrode plates for the present prototype are made of bakelite paper laminates of dimensions $27\text{ cm} \times 27\text{ cm}$ and thickness of 2 mm each having bulk resistivity $\sim 3 \times 10^{10}\ \Omega\text{ cm}$ at 25°C . Before making the gas gap, a thin layer of linseed oil coating is applied to the inner surfaces of the electrode plates to make the surface smooth. The coating thickness is $\sim 30\ \mu\text{m}$. The linseed oil is cured for about 15 days and checked visually whether the oil is dried out completely. Four edge spacers of dimensions $27\text{ cm} \times 1\text{ cm}$ and one button spacer of diameter 1 cm are used for making the uniform gas gap. Two gas inlets and outlet nozzles are placed along with the edge spacers at diagonal corners. All the spacers and gas nozzles are made of polycarbonate (bulk resistivity $\sim 10^{15}\ \Omega\text{ cm}$) and have a thickness of 2 mm. The average surface resistivity of the two outer surfaces graphite layers are measured to be $\sim 510\text{ k}\Omega/\square$ and $\sim 540\text{ k}\Omega/\square$ respectively. High voltage (HV) of equal and opposite polarities are applied on the diagonally opposite corners of the two outer surfaces of the detector.

Signals are collected using 2.5 mm wide copper strips. The separation between two strips are kept 2 mm. The signals from the strips are collected through RG-174/U coaxial cables. A more detailed illustration of the fabrication procedure can be found in the Ref [22].

3 Experimental set-up

In this work the efficiency, noise rate, time resolution, charge sharing of the prototype are measured using cosmic ray. The long-term stability of the

chamber is tested. The efficiency of the chamber is also measured in a high gamma ray background in the laboratory using ^{137}Cs source.

To generate the cosmic ray trigger, an array of three plastic scintillation detectors is used. On top of the RPC, a scintillator of dimension $10\text{ cm} \times 10\text{ cm}$ (SC1) and a finger scintillator of dimension $10\text{ cm} \times 2\text{ cm}$ (SC2) are placed, and at the bottom, the paddle scintillator of dimension $20\text{ cm} \times 20\text{ cm}$ (SC3) is placed as shown in Figure 1. The separation between the SC1 and SC2 is kept 5 cm whereas the distance between SC2 and RPC and RPC and SC3 are kept at 3 cm and 4 cm respectively. +1550 V is applied to each PMT for the operation of the scintillators. -15 mV threshold is applied to the Leading Edge Discriminator (LED) for each scintillation detector. Discriminated signals from three scintillation detectors are taken in coincidence to generate the 3-fold trigger (master trigger).

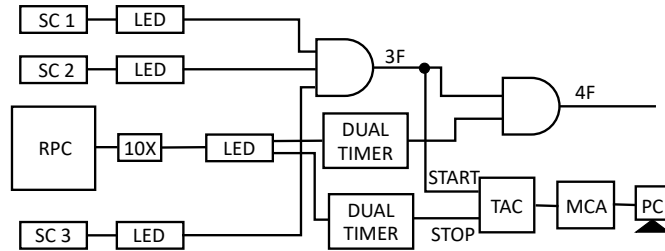


Figure 1: Block diagram of the cosmic ray test setup for the measurement of efficiency and time resolution. SC1, SC2 and SC3 are the plastic scintillators of dimensions $10\text{ cm} \times 10\text{ cm}$, $10\text{ cm} \times 2\text{ cm}$ and $20\text{ cm} \times 20\text{ cm}$ respectively. The distance between SC1 and SC2, SC2 and RPC, and RPC and SC3 are kept at 5 cm, 3 cm and 4 cm respectively. 10X, LED, TAC, MCA, PC are the 10X fast amplifier, Leading Edge Discriminator, Time to Amplitude Converter, Multi-Channel Analyser and Personal Computer respectively.

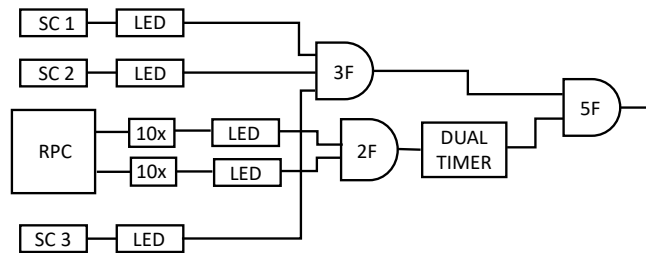


Figure 2: Block diagram of the setup for charge sharing measurement.

The signal from the RPC pickup strip is fed to a 10X fast amplifier and the amplifier signal goes to the LED. One output from the LED goes to the scalar counter for the singles count or the noise count of the detector.

For a finite time interval the counts from one single RPC strip is stored in the scalar. When the number is divided by the time interval and the area of the strip the single count rate is found in unit of Hz/cm². The other output from the LED is fed to a Dual Timer where the discriminated RPC signal is stretched to 500 ns to avoid any double or multiple counting of the signals and also to apply proper delay to match the RPC signal with the 3-fold trigger. The output of the dual timer is finally fed to the logic module to get the 4-fold signal generated in coincidence with the 3-fold trigger. The ratio of the 4-fold signal to the 3-fold trigger signal is defined as the efficiency. The area of coincidence window of the cosmic ray test-bench is 10 cm × 2 cm.

To measure the time resolution of the detector, the 3-fold trigger signal is used as the START signal of the Time to Amplitude Converter (TAC) and the dual timer output (as shown in Figure 1) is used as the STOP input signal of the TAC. The output of the TAC is further fed to the Multi-Channel Analyser (MCA), and MCA is connected to the Personal Computer (PC) to store the timing spectra. 100% C₂H₂F₄ gas is used as the active medium during the study of the timing properties. The temperature and the humidity are also recorded during the entire measurements using a data logger, built-in house [24].

For measurement of charge sharing, signals from two consecutive strips are taken in coincidence as shown in the Figure 2. The amplified and discriminated RPC signals from two consecutive strips are first sent to the coincidence logic and the logic output (2F) is fed to the dual timer for the proper delay matching. Dual timer output is then taken in coincidence with the trigger generated by 3-fold scintillator array to make 5F. The ratio of the 5F count to the 3F count is defined as the charge sharing.

For the radiation hardness measurement, a strong ¹³⁷Cs (662 keV gamma) source of activity 13.6 GBq is used.

4 Result

The detector is first tested with the 100% C₂H₂F₄ gas using cosmic ray. Efficiency plateau ~ 95% from 9.4 kV onwards and ~ 85% from 10.1 kV onwards are obtained for -15 mV and -20 mV discriminator threshold settings respectively. The noise rate measured is very high for the lower threshold with a maximum value of ~ 500 Hz/cm² for the prototype [22].

The detector is further tested in the avalanche mode with a more conventional gas mixture of C₂H₂F₄ and i-C₄H₁₀ in the 90/10 volume ratio. Isobutane has a high UV absorption coefficient, and it prevents the formation of secondary discharges due to photoelectrons. The performance is even better with the application of an additional quencher. Both the current and noise rate are very low for this gas mixture compared to that with the 100%

$C_2H_2F_4$ used for the same detector. An efficiency of greater than 90% is achieved from 10 kV onwards for both - 20 mV and - 25 mV threshold settings. The maximum noise rates are found to be 120 Hz/cm² and 80 Hz/cm² for the - 20 mV and - 25 mV thresholds, respectively. The detailed I-V characteristics, efficiency, and noise rate results are elaborated in the article [23].

To measure the timing properties, the RPC signal is stretched to 500 ns. Full scale of the TAC is set to 100 ns. The START signal of the TAC is taken from the 3-fold scintillator trigger and the STOP signal is taken from the RPC. The typical time spectrum at 10.2 kV for the RPC with 100% $C_2H_2F_4$ gas is shown in Figure 3. The distribution of the time difference between the master trigger and the RPC signal is fitted with the Gaussian function. The σ_{tot} of the distribution is found out and subtracting the contribution of the scintillators (σ_{SC}) in quadrature the intrinsic time resolution (σ) of the RPC detector is calculated using the formula;

$$\sigma = \sqrt{\sigma_{tot}^2 - \sigma_{SC}^2} \quad (1)$$

At 10.2 kV the σ_{tot} is found to be 0.96 ± 0.05 ns as shown in Figure 3. The measurement is repeated for five different voltage settings.

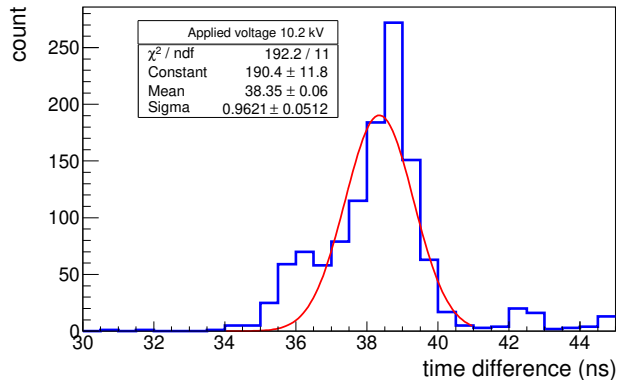


Figure 3: Time spectrum of RPC at an applied voltage difference of 10.2 kV across the gas gap.

The intrinsic time resolution (σ) of the RPC as a function of the applied voltage is shown in Figure 4. With the increase of applied voltage σ improves. At 10.4 kV, the optimum time resolution is found to be ~ 0.8 ns. It is to be mentioned here that previously for a prototype made with the same material but without oil coating, the resolution was found to be ~ 1.2 ns at 10.2 kV [25].

Charge sharing is measured between the two consecutive readout strips varying the applied voltage with the $C_2H_2F_4$ and $i-C_4H_{10}$ gas mixture. As

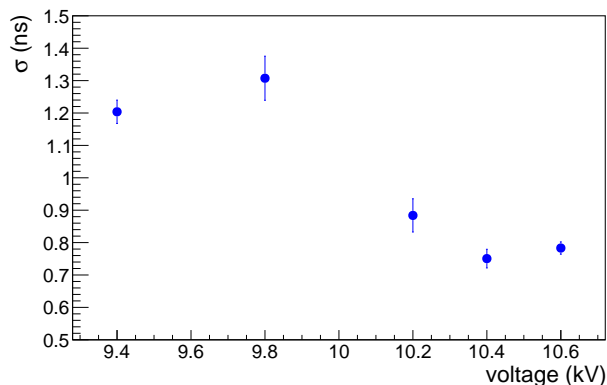


Figure 4: Time resolution (σ) of the RPC as a function of applied voltage.

mentioned earlier the charge sharing is defined as the ratio of the coincidence count of two consecutive readout strips taken in coincidence with the 3F scintillator trigger (5F) to the trigger count (3F). Actually, for this measurement the finger scintillator of the trigger is placed just above one single strip and from which the efficiency is also measured for reference.

The charge sharing between two consecutive strips as a function of applied voltage is shown in Figure 5. In the same plot the efficiency as a function of voltage measured on the same day is also shown for reference. One can see in Figure 5 that the shared charge is about $\sim 30\%$, where the efficiency measured from a single strip is $\sim 90\%$. With the increasing voltage the shared charge initially increased and then remained constant within the error bars. Although we have referred this measurement as charge sharing but the crosstalk between the two strips are not eliminated for this particular measurement.

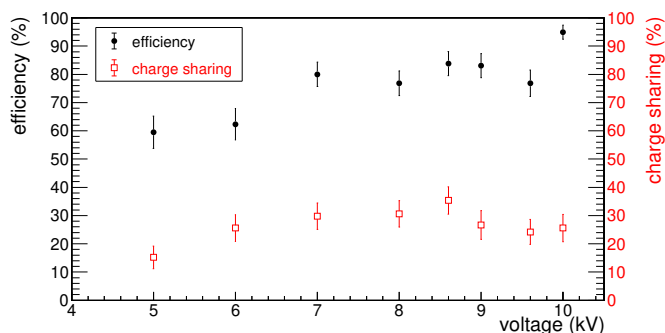


Figure 5: Variation of efficiency and shared charge between two consecutive strips with the voltage.

Finally, the prototype is tested in the high intensity gamma ray envi-

ronment. A ^{137}Cs source of activity ~ 13.6 GBq is used for the this measurement. 662 keV photons are emitted from the source with a measured flux of ~ 46 kHz/cm 2 . As shown in Figure 6 the source is placed on the top of the top scintillator paddle. The efficiency is measured for the voltage setting of 10.2 kV with and without the gamma source. The measurement is performed with the $\text{C}_2\text{H}_2\text{F}_4$ and $i\text{-C}_4\text{H}_{10}$ gas mixture in the 90/10 volume ratio. The obtained efficiency value is shown in absence and presence of the gamma source in Figure 7. It is observed that the efficiency decreased by only 1 % with a gamma ray flux of 46 kHz/cm 2 from the efficiency value without the source.

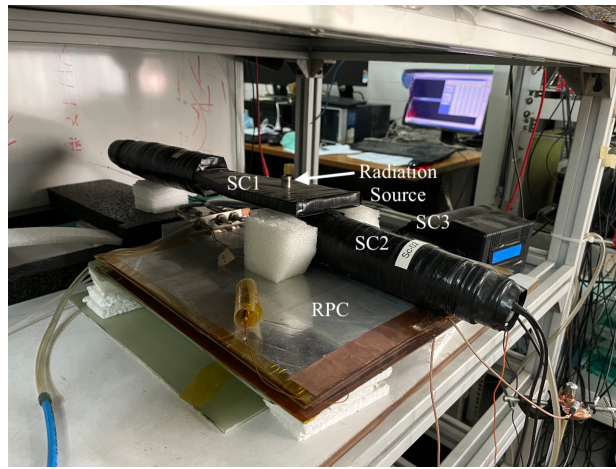


Figure 6: Setup to measure the efficiency in presence of high intensity gamma ray flux.

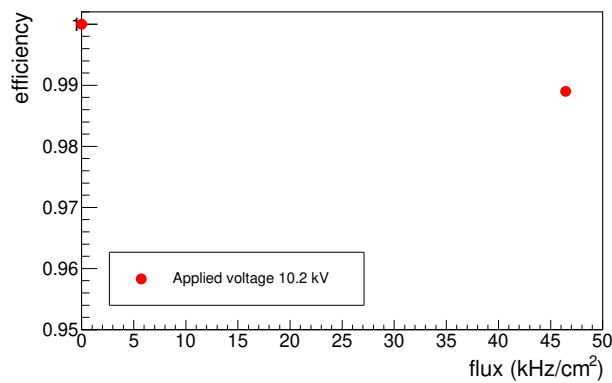


Figure 7: Efficiency in presence and absence of high intensity gamma ray flux at an applied voltage difference of 10.2 kV across the gas gap.

The detector is also tested for long-term with cosmic rays. During the

long-term operation the detector is operated with two types of gas mixture. One is with 100% $C_2H_2F_4$ gas and another is with $C_2H_2F_4$ and $i-C_4H_{10}$ mixture in the 90/10 volume ratio. Initially, the detector is operated with a mixture of $C_2H_2F_4$ and $i-C_4H_{10}$ and then it is continuously tested with 100% $C_2H_2F_4$ for next few days. After that it is again tested with the mixed gas.

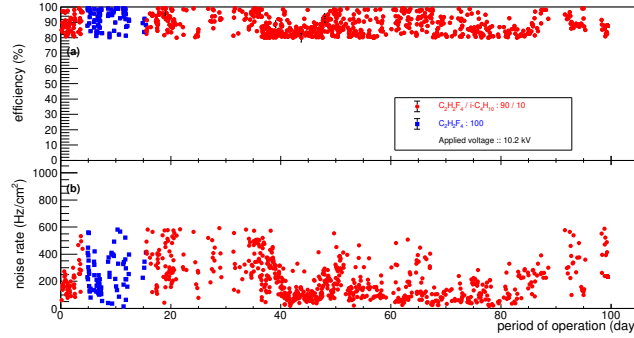


Figure 8: (a) Efficiency and (b) noise rate of the detector as a function of period of operation for two different gas compositions at applied voltage of 10.2 kV. For some data points the error bars are smaller than the size of the markers.

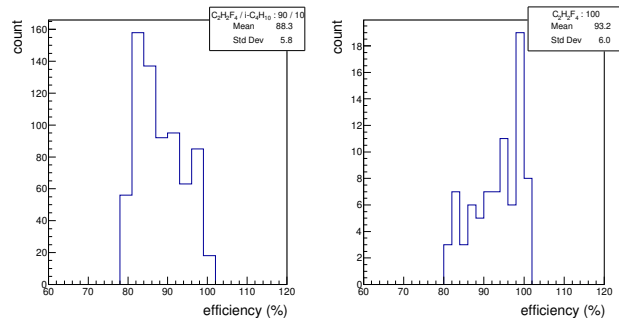


Figure 9: Distribution of the efficiency values of long-term measurements at applied voltage of 10.2 kV.

The measured efficiency and noise rate of the detector as a function of the period of operation for two different gas compositions are shown in Figure 8. The distribution of efficiency and noise rate for two gas compositions are shown in Figure 9 and 10 respectively. The detector is tested for more than 90 days.

It is found that for $C_2H_2F_4$ and $i-C_4H_{10}$ mixture and 100% $C_2H_2F_4$ the average efficiencies are found to be 88 ± 6 % and 93 ± 6 % respectively whereas the average noise rates for two compositions are found to

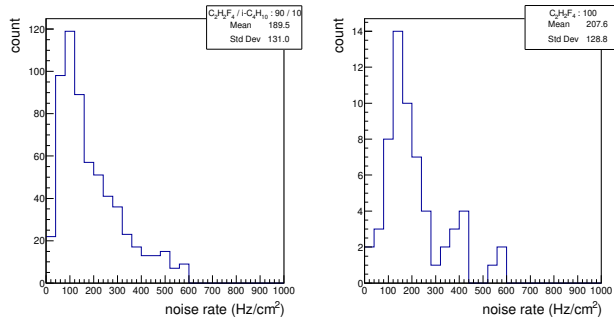


Figure 10: Distribution of the noise rate values of long-term measurements at applied voltage of 10.2 kV.

be 189 ± 131 Hz/cm² and 208 ± 129 Hz/cm². The long-term stability is studied for about 100 days.

5 Summary and outlook

A RPC prototype made of linseed oil coated indigenous bakelite material of thickness 2 mm and having bulk resistivity $\sim 3 \times 10^{10}$ Ω cm is tested.

The detector is tested initially with 100% C₂H₂F₄ gas in the avalanche mode. With the applied voltage of 10.4 kV onwards, the time resolution obtained is ~ 0.8 ns. The time resolution of the module is also comparable with that of the conventional linseed oil-coated bakelite RPC.

Variation of charge sharing between the consecutive strips is measured with the applied voltage. From 5 to 8 kV the shared charge initially increased and reached a constant ($\sim 30\%$) within the error bar. With the increasing voltage shared charge has not increased further and remained constant with a little fluctuations.

The preliminary stability test of the chamber is performed using C₂H₂F₄ and i-C₄H₁₀ mixture and 100% C₂H₂F₄ for about 100 days. The overall efficiency for the entire period is found to be $\sim 90\%$.

This radiation tolerance test is very important for an experiment, especially for high-energy physics experiments where detectors are subjected to continuous operation at high rate environment for a long time. For the present prototype a very good efficiency is obtained where it is operated in the presence of a high-intensity photon source. It is also observed that the efficiency decreased by only 1 % from the efficiency value without the source with a gamma ray flux of 46 kHz/cm².

6 Acknowledgements

The authors would like to thank Prof. Sanjay K. Ghosh and Dr. Sidharth K. Prasad for their valuable discussions and suggestions during the course of the study. Dr. Somen Gope of Bose Institute is acknowledged for some help during the measurements. We would also like to thank Dr. Sumit Kumar Kundu, Indiana University, Bloomington, USA ; Mr. Ayan Dandapat of IIT Ropar, Punjab, India ; and Mr. Pranjal Barik of Savitribai Phule Pune University, Pune, India, for their help during data taking. Mr. Subrata Das is acknowledged for helping in the fabrication of the pick-up strips used in this study. This work is partially supported by the CBM-MuCh project from BI-IFCC, DST, Govt. of India. A. Sen acknowledges his Inspire Fellowship research grant [DST/INSPIRE Fellowship/2018/IF180361].

References

- [1] R. Santonico and R. Cardarelli, Nucl. Inst. and Meth. A **187** (1981) 377.
- [2] S. Biswas *et al.*, Nucl. Inst. and Meth. A **617** (2010) 138.
- [3] S. K. Park *et al.*, 2012 JINST **7** P11013.
- [4] A. D. Bhatt *et al.*, Nucl. Inst. and Meth. A **844** (2017) 53.
- [5] F. Anulli *et al.*, Nuclear Physics B (Proc. Suppl.) 61B (1998) 244.
- [6] The ATLAS collaboration *et al.* 2021 JINST 16 P07029.
- [7] A. Ferretti *et al.* 2019 JINST 14 C06011.
- [8] M. Spegel *et al.* Nucl. Inst. and Meth. A **453** (2000) 308.
- [9] E. Cerron Zeballos *et al.*, Nucl. Instr. and Meth. A **374** (1996) 132.
- [10] P Bernardini and (for the ARGO-YBJ Collaboration) 2008 J. Phys.: Conf. Ser. **120** 062022.
- [11] G.A. Agnetta *et al.*, Nucl. Instr. and Meth. A **381** (1996) 64.
- [12] Q. Zhang *et al.*, Nucl. Instr. and Meth. A **583** (2007) 278.
- [13] C. Lu, Nucl. Instr. and Meth. A **602** (2009) 761.
- [14] M. Abbrescia *et al.*, Nucl. Instr. and Meth. A **394** (1997) 13.
- [15] B. Hong *et al.*, Journal of the Korean Physical Society, Vol. 48, No. 4, April 2006, 515.

- [16] BaBar Technical Design Report, BaBar Collaboration, SLAC Report SLAC-R-95-457, March 1995.
- [17] F. Anulli *et al.*, Nucl. Instr. and Meth. A **508** (2003) 128.
- [18] G. Cattani, Journal of Physics: Conference Series **280** (2011) 012001.
- [19] S. Park *et al.*, Nucl. Instr. and Meth. A **550** (2005) 551
- [20] J. Zhang *et al.*, Nucl. Instr. and Meth. A **540** (2005) 102.
- [21] S. Biswas *et al.*, Nucl. Instr. and Meth. A **604** (2009) 310.
- [22] A. Sen *et al.*, Nucl. Instrum. Methods. A **1024** (2022) 166095.
- [23] A. Sen *et al.*, Nucl. Instrum. Methods. A **1045** (2023) 167572.
- [24] S. Sahu *et al.*, JINST **12** (2017) C05006.
- [25] A. Sen *et al.*, JINST **15** (2020) C06055.